# INVESTIGATION OF SEISMIC RECORDS OF THE 2011 OFF THE PACIFIC COAST OF TOHOKU EARTHQUAKE AT A DAM SITE USING THE EMPIRICAL GREEN'S FUNCTION METHOD

Hiroshi ASAHARA[1], Masayuki KASHIWAYANAGI[2] and Tsuneo OHSUMI[3]

[1] Department of Civil and Environmental Engineering, Graduate School of Advanced Technology of Science, The University of Tokushima, Tokushima, Japan, asahara@astom.co.jp
[2] Adviser, Civil Planning & Design Office, Civil & Electrical Engineering Department, Electric Power Development Co., Ltd., Tokyo, Japan, masayuki_kashiwayanagi@jpower.co.jp
[3] Professor, Department of Civil and Environmental Engineering, Graduate School of Advanced Technology of Science, The University of Tokushima, Tokushima, Japan, t_ohsumi@ce.tokushima-u.ac.jp

**ABSTRACT**: Seismic waveforms of the 2011 off the Pacific coast of Tohoku Earthquake recorded at the base of a dam site in Fukushima prefecture are reproduced based on the empirical Green's function method. Three empirical Green's functions are prepared to five strong-motion-generation-areas (SMGAs) model. The shape and peak acceleration of the observed waveform are roughly explained. Nearly simultaneous arrivals from SMGAs at off-shore Miyagi prefecture and off-shore Fukushima prefecture contributed to the maximum acceleration value at the target site.

**Key Words**: empirical Green's function method, the 2011 off the Pacific coast of Tohoku Earthquake, aftershock, dam site

## INTRODUCTION

Dam sites located in Tohoku area have recorded many seismic waveforms of the 2011 off the Pacific coast of Tohoku Earthquake, Japan, which occurred on March 11, 2011 (main shock, $M_w$ 9.0) and its aftershocks. Several kinds of rupture processes of the main shock have been proposed using teleseismic waveforms (e.g., Ide *et al*., 2011, Ammon *et al*., 2011) or strong motions (e.g., Furumura *et al*., 2011, Kurahashi and Irikura, 2011). It is common that every rupture model shows complex rupture propagation though the results vary from the focused frequencies or the analysis methods. The authors reproduced the waveforms of the main shock using the empirical Green's function (EGF) method (Irikura, 1986).

The EGF method is a technique to synthesize seismic records of a large event using the recorded data at small events as Green's functions. After the second proposal of Japan Society of Civil Engineering (JSCE), following the Southern Hyogo prefecture earthquake in 1995, simulation of earthquake ground motions using the Green's function approach for a potential rupturing fault, has been included in one of the seismic resistant design codes (JSCE, 1996). Since the EGF method mainly depends on and uses small ground motion histories, small events selected as Green's functions are necessary to share the same path and site effects with the target event. Seismic waveforms recorded at the base of dam sites are suitable for this analysis, where seismic motion is less affected by sedimentary layers. Seismic records at the base of dam sites are affected by the structure above at high frequency range, whereas show the characteristics similar to those on the bedrock at frequency range approximately lower than 1 Hz.

The authors reproduced the waveform of the main shock by the EGF method using waveforms of small events as the Green's functions. The influence rate of rupture processes to the waveforms was discussed, comparing the synthesized data and the recorded waveform.

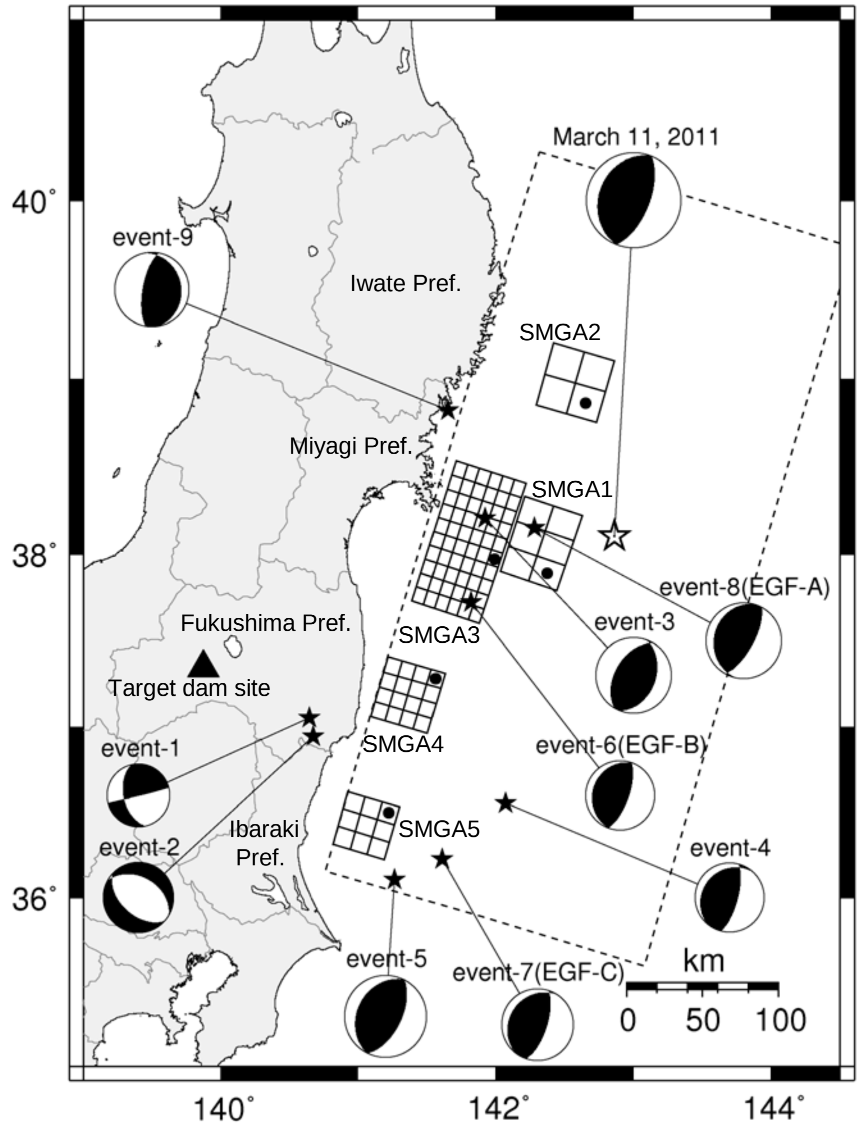


Fig.1 The location of the target dam site (filled triangle), the fault zone (large dashed rectangle), characterized source model consisting of five SMGAs in the fault zone (small solid rectangles). The small rectangles and the closed circles inside them show the SMGAs and their initiation points. The open star and the closed stars show the epicenters of the main shock and the small events which are candidates for EGFs, respectively. EGF-A, B and C are selected as EGFs.

Table 1 The source parameters of the main shock and the small events which are candidates for EGFs. The origin times and the locations were determined by JMA. The CMT solutions and moments were reported by F-net. Stress drops and areas for EGFs were determined in this study.

| | Origin time | Latitude (deg) | Longitude (deg) | Depth (km) | $M_W$ | Strike (deg) | Dip (deg) | Rake (deg) | $M_0$ (N m) | Stress drop (MPa) | Area ($km^2$) |
|---|---|---|---|---|---|---|---|---|---|---|---|
| Main shock | 2011/03/11 14:46:18.12 | 38.103 | 142.861 | 23.7 | 9.0 | 22/200 | 91/88 | 63/27 | 1.07E+22 | | |
| Event-1 | 2011/04/12 14:07:42.28 | 37.053 | 140.643 | 15.1 | 5.9 | 76/167 | 89/51 | 141/2 | 7.05E+17 | | |
| Event-2 | 2011/04/12 17:16:12.02 | 36.946 | 140.673 | 6.4 | 6.6 | 132/301 | 50/41 | -82/-99 | 9.58E+18 | | |
| Event-3 | 2011/04/07 23:32:43.46 | 38.204 | 141.920 | 65.9 | 7.1 | 211/20 | 50/40 | 97/81 | 4.74E+19 | | |
| Event-4 | 2011/03/11 16:14:56.80 | 36.555 | 142.069 | 20.0 | 6.5 | 15/220 | 71/21 | 81/113 | 6.16E+18 | | |
| Event-5 | 2011/03/11 15:15:34.47 | 36.108 | 141.265 | 43.2 | 7.8 | 26/209 | 59/31 | 89/92 | 5.66E+20 | | |
| Event-6 (EGF-B) | 2010/03/14 17:08:04.18 | 37.724 | 141.818 | 39.8 | 6.5 | 20/199 | 69/21 | 91/89 | 6.83E+18 | 21.2 | 84.6 |
| Event-7 (EGF-C) | 2008/05/08 01:45:18.77 | 36.228 | 141.608 | 50.6 | 6.8 | 18/216 | 68/24 | 83/107 | 1.97E+19 | 31.2 | 132 |
| Event-8 (EGF-A) | 2005/08/16 11:46:25.74 | 38.150 | 142.278 | 42.0 | 7.1 | 29/194 | 69/22 | 96/76 | 5.43E+19 | 21.3 | 339 |
| Event-9 | 2003/05/26 18:24:33.42 | 38.821 | 141.651 | 72.0 | 7.0 | 190/350 | 69/22 | 97/71 | 3.49E+19 | | |

## WAVEFORM REPRODUCTION OF THE MAIN SHOCK

The target dam site is located in the Tohoku area, and the location is marked by a filled triangle in Fig. 1. This dam is a rock-fill dam. Seismographs are installed at the tops and the base of the dam. This site has recorded seismic waves of the main shock and its aftershocks. Seismic waveforms of horizontal upstream-downstream (orthogonal to the enclosing bund) component recorded at the base of the dam site were used in this study.

To simulate strong motions using EGF method, the characterized source model and the EGFs are needed. The characterized source model was constructed using Kurahashi and Irikura (2011) model, which consists of five strong-motion-generation-areas (SMGAs). EGFs were selected from the aftershock records and the past records prior to the main shock, considering the propagation path and the radiation characteristic from the source.

### Selection of the EGF

The target dam site has 9 seismic records other than that of the main shock, whose record length exceed 40 seconds and whose epicenters are inside or around the fault zone of the main shock. These 9 records are the candidates for EGFs. The hypocenters and CMT solutions of these records are shown in Fig. 1. The source parameters of the main shock and the small events reported by the Japan Meteorological Agency (JMA) and the CMT solutions reported by F-net (Okada *et al*., 2004) are shown in Table 1. Event-1 to -5 occurred after the main shock, whereas event-6 to -9 occurred prior to the main shock.

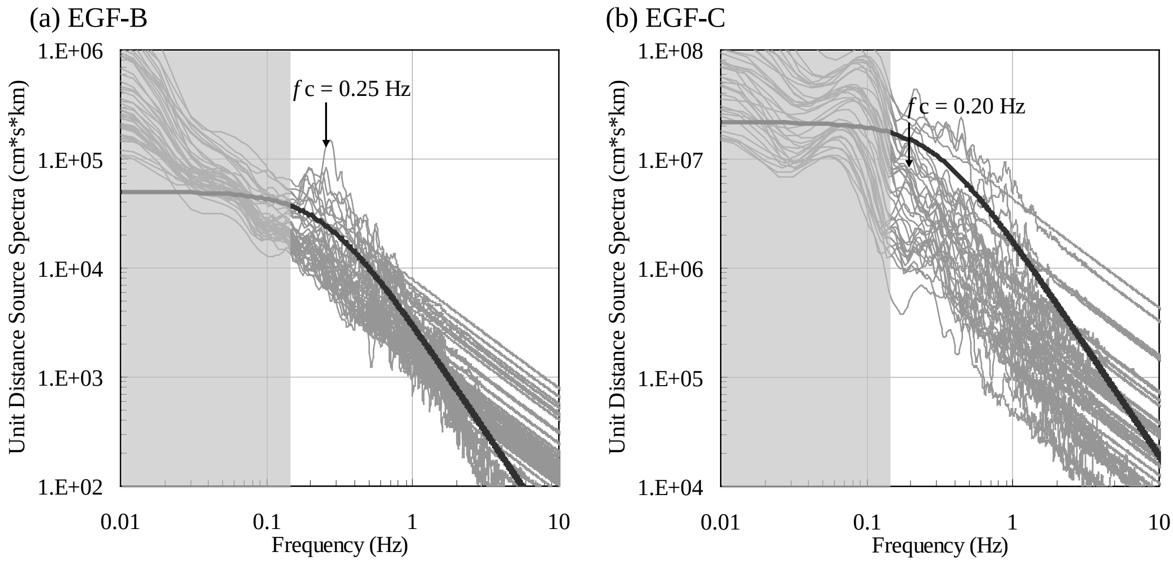


Fig. 2 Displacement spectra estimated from bore-hole motion records at KiK-net stations on rock from the small events ((a) EGF-B and (b) EGF-C) used as the empirical Green's functions. The shadow areas at low frequencies lower than 0.15 Hz show unreliable frequency range that was not used for the simulation.

The small events' records used as EGFs have to share the propagation path and site effects as well as the radiation characteristic from the source. Event-8 (August 16, 2005, $M_w$ 7.1) was commonly selected as the EGF for SMGA 1 and 2. We call this event as EGF-A. In a similar way, event-6 (March 14, 2010, $M_w$ 6.5) was selected as the EGF for SMGA 3 and 4 (EGF-B), and event-7 (May 8, 2008, $M_w$ 6.8) was selected for SMGA 5 (EGF-C). Event-3 was not selected as an EGF, on the grounds that this event was not an inter-plate earthquake but an intra-slab one (Ohta *et al*., 2011), although the epicenter was inside the fault zone. The moment magnitude of event-5 ($M_W$ 7.8) was too large to use as EGF.

The information of stress drop and fault area is needed to use the waveforms as EGF. The corner frequencies of EGF-B and EGF-C were estimated using bore-hole motion records of KiK-net (Aoi *et al*., 2000) as shown in Fig. 2. The stress drop of these small events was calculated from the corner frequency and seismic moment relation (Boore, 1983). The fault area of the small event was obtained by the circular clack model by Brune (1970, 1971). Conversely, the source models of EGF-A had been estimated (e.g., Kamae, 2006, Suzuki and Iwata, 2007). The estimated models showed that this earthquake consisted of two large slips. We decided the fault size of EGF-A considering total size of large slips. Stress drop was obtained from the size and seismic moment using the circular crack formula (Eshelby, 1957). In this study, the observed records used as the EGFs were band-pass-filtered from 0.15 Hz to 10 Hz, considering the reliable frequency range of the observed records.

## Characterized Source Model and Ground Motion Simulation

The characterized source model was constructed using Kurahashi and Irikura (2011) model, slightly modifying the source parameters for our EGFs. The source parameters of each SMGA, such as the length, width, seismic moment, stress drop and delay time from the origin time of each SMGA are listed in Table 2. To calculate ground motions from each SMGA, the area of the SMGA was divided into equally-sized square sub faults, the area of which was set to be the same as the small events area as shown in Fig. 1. SMGA 1 and SMGA 3 are located off-shore Miyagi prefecture. SMGA 2, SMGA 4 and SMGA 5 are located off-shore Iwate prefecture, Fukushima prefecture and Ibaraki prefecture,

Table 2 The source parameters of each SMGA.

| | SMGA 1 | SMGA 2 | SMGA 3 | SMGA 4 | SMGA 5 |
|---|---|---|---|---|---|
| $L$ (km) | 55.2 | 36.8 | 92.0 | 36.8 | 34.5 |
| $W$ (km) | 36.8 | 36.8 | 55.2 | 36.8 | 34.5 |
| $N_L \times N_W \times N_D$ | 3×2×7 | 2×2×3 | 10×6×11 | 4×4×4 | 3×3×2 |
| $M_0$ (N m) | 2.28E+21 | 6.52E+20 | 4.51E+21 | 4.37E+20 | 3.55E+20 |
| Stress drop (MPa) | 39.9 | 23.4 | 29.7 | 16.3 | 25.9 |
| Delay time from origin time (sec) | 15.64 | 66.42 | 68.41 | 109.71 | 118.17 |
| Rise time (sec) | 3.3 | 3.3 | 4.9 | 3.3 | 3.1 |
| EGF | EGF-A | EGF-A | EGF-B | EGF-B | EGF-C |

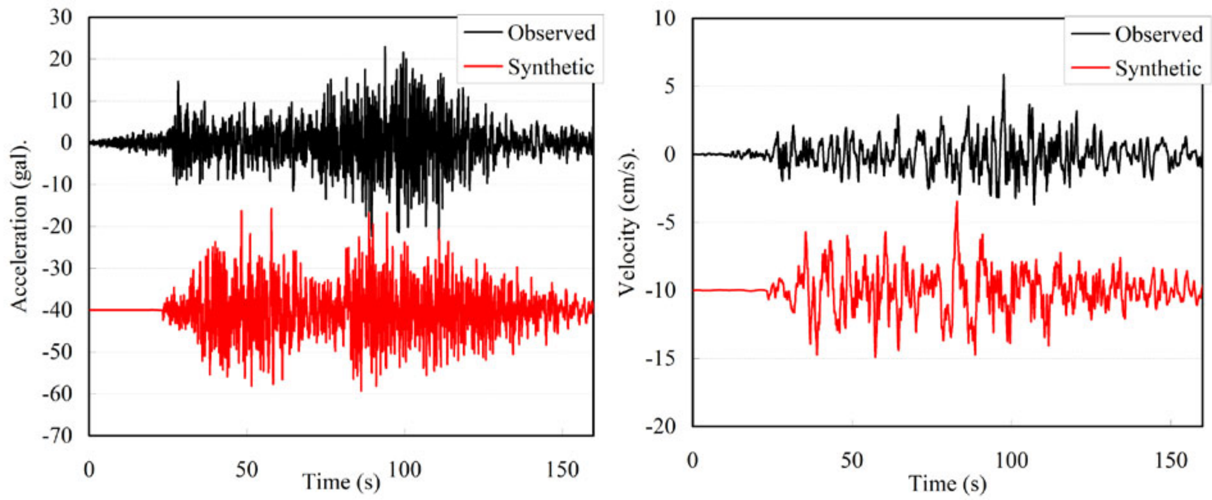


Fig.3 Comparison of the observed (black traces) and synthetic (red traces) seismographs by the EGF method at the dam site. The acceleration (left) and velocity (right) are composed.

respectively.

The rise times inside each SMGA were given by the empirical relations by Kataoka *et al*. (2003). The average S wave velocity and the rupture velocity were given to be 3.5 km/s and 2.8 km/s, respectively. The $Q_S$ value for plate boundary earthquakes in Eastern Japan area, which was proposed by Kawase and Matsuo (2004), was used as the propagation property at this area; $Q_S = 93 f^{0.89}$. Here $f$ is frequency (Hz).

## DISCUSSION

The observed and synthetic waveforms (acceleration and velocity) at the dam site are shown in Fig. 3. The base time at these graphs is the start time of the observed, 58 seconds after the origin time. The shape and peak acceleration of the observed waveform were roughly explained by the synthetic using five SMGAs. The observed peak acceleration was 23 gal, whereas the synthetic peak was 24 gal. The acceleration waveforms had two peaks: the first appeared around 30 sec. and the second appeared around 100 sec. The synthetic first peak was calculated larger than that of the observed, though the

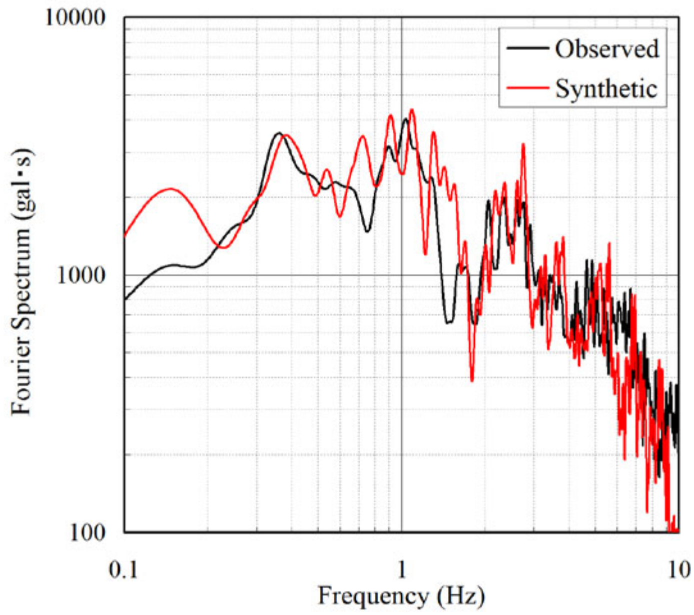


Fig.4 Fourier spectra of observed (black trace) and synthetic (red trace) accelerations shown in Fig. 3.

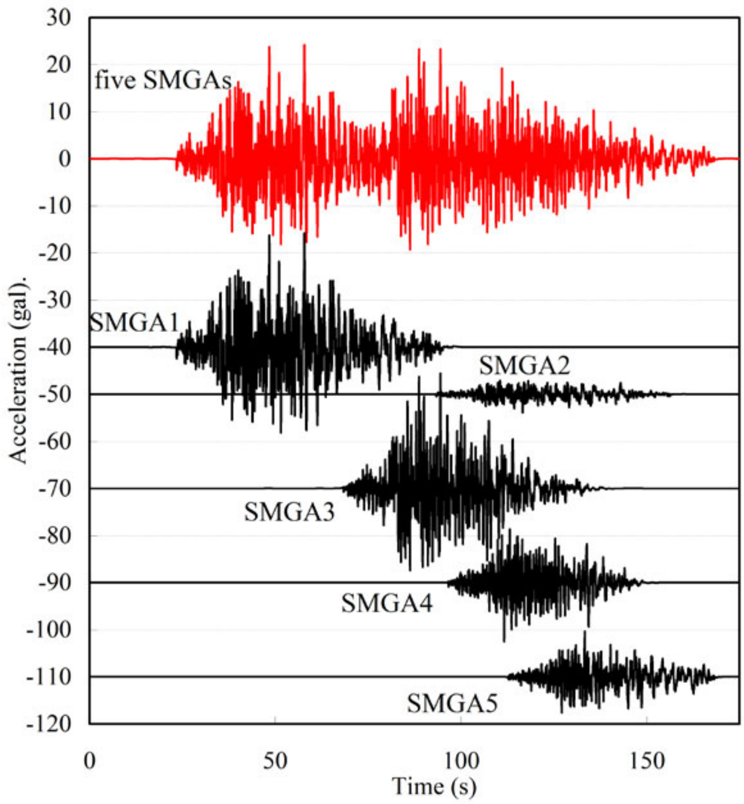


Fig.5 Comparison of synthetic waveforms from five SMGAs (red trace) and from individual SMGAs (black traces) from SMGA1 to SMGA5.

synthetic second peak was similar to that of the observed. The initial tremor of the observed was not recreated on the grounds that the EGF data started just before the S wave arrival, lacking the initial P wave data because of the specification of the observation system.

The observed and synthetic Fourier spectra are shown in Fig. 4. The synthetic Fourier spectrum was well consistent with the observed at all frequency range. The observed and synthetic had commonly peaks at about 0.4 Hz and 1.0 Hz, and bottom at 1.8Hz. The observed bottom at 1.5 Hz was not recreated.

The waveforms synthesized from individual SMGAs were shown in Fig. 5. The waveform before 70 sec. only depended on SMGA1, and SMGA2 had a little impact on the waveform. The low acceleration period between the first and second peaks showed the interval between SMGA1 and SMGA3. The influences from SMGA 3 to 5 reached in sequence. Comparing waveforms of individual SMGAs with the observed waveform, it was found that SMGA3 and SMGA4 had the largest influence on the waveform. Though the fracture start times of these SMGAs were about 40 seconds away, the arrival times at the target site were came closer. The nearly arrivals made the peak acceleration around 100 sec.

## CONCLUSIONS

The seismic waveform of the 2011 off the Pacific coast of Tohoku Earthquake recorded at the target dam site was reproduced using the empirical Green's function method. Three empirical Green's functions were prepared to five SMGAs. The shape and peak acceleration of the observed waveform were roughly explained by the model using five SMGAs. The comparison of the observed and synthetic waves made it clear that nearly simultaneous arrivals of wave packets from SMGAs at off-shore Miyagi and off-shore Fukushima contributed to the maximum acceleration value at the site.

## ACKNOWLEDGMENTS

The authors are grateful to the National Institute for Earth Science and Disaster Prevention (NIED), Japan for providing strong motion data of the KiK-NET and the CMT solutions by the F-net.

## REFERENCES

Ammon, C. J., Lay, T., Kanamori, H. and Cleveland, M. (2011). "A rupture model of the 2011 off the Pacific coast of Tohoku Earthquake." *Earth Planets Space,* Vol. 63, 693 – 696.

Aoi, S., Obara, K., Hori, S., Kasahara, K. and Okada, Y. (2000). "New strong-motion observation network: KiK-net." *Eos Transactions AGU, Fall Meeting Suppl., Abstract* S71A-05.

Boore, D.M. (1983). "Stochastic simulation of high-frequency ground motions based on seismological models of the radiated spectra." *Bulletin of the Seismological Society of America*, Vol. 73, No. 6, 1865 – 1894.

Brune, J.N. (1970). "Tectonic stress and the spectra of seismic shear waves from earthquakes." *Journal of Geophysical Research*, Vol. 75, No. 26, 4997 – 5009.

Brune, J.N. (1971). "Correction." *Journal of Geophysical Research*, Vol. 76, No. 20, 5002.

Eshelby, J.D. (1957). "The determination of the elastic field of an ellipsoidal inclusion, and related problems." *Proceedings of the Royal Society A*, Vol. 241, No. 1226, 376 – 396.

Furumura, T., Takemura, S., Noguchi, S., Takemoto, T., Maeda, T., Iwai, K. and Padhy, S. (2011) "Strong ground motions from the 2011 off-the Pacific-Coast-of-Tohoku, Japan (Mw = 9.0) earthquake obtained from a dense nationwide seismic network." *Landslides,* Vol. 8, 333 – 338.

Ide, S., Baltay, A. and Beroza, G. C. (2011). "Shallow Dynamic Overshoot and Energetic Deep Rupture in the 2011 $M_W$ 9.0 Tohoku-Oki Earthquake." *Science*, Vol. 332, No. 6036, 1426 – 1429.

Irikura, K. (1986). “Prediction of strong acceleration motion using empirical Green’s function.” *Proceeding of 7th Japan Earthquake Symposium*, 151 – 156.

Japan Soceiety of Civil Engineering (1996). “*Proposal on earthquake resistance of civil engineering structrures.*”

Kamae, K. (2006). “Source modeling of the 2005 off-shore Miyagi prefecture, Japan, earthquake ($M_{JMA}$=7.2) using the empirical Green’s function method.” *Earth Planets Space*, Vol. 58, 1561 – 1566.

Kataoka, S., Kusakabe, T., Murakoshi, J. and Tamura, K. (2003). “Study on a Procedure for Formulating Level 2 Earthquake Motion Based on Scenario Earthquakes.” *Research Report of National Institute for Land and Infrastructure Management*, 15.

Kawase, H. and Matsuo, H. (2004). “Separation of Source, Path and Site Effects based on the Observed Data by K-NET, KiK-net, and JMA Strong Motion Network.” *Journal of JAEE*, Vol. 4, No. 1, 33 – 52.

Kurahashi, S. and Irikura, K. (2011). “Source model for generating strong ground motions during the 2011 off the Pacific coast of Tohoku Earthquake.” *Earth Planets Space*, Vol. 63, 571 – 576.

Ohta, Y., Miura, S., Ohzono, M., Kita, S., Iinuma, T., Demachi, T., Tachibana, K., Nakayama, T., Hirahara, S., Suzuki, S., Sato, T., Uchida, N., Hasegawa, A. And Umino, N. (2011). “Large intraslab earthquake (2011 April 7 M7.1) after the 2011 off the Pacific coast of Tohoku earthquake (M9.0): Coseismic fault model based on the dense GPS network data.” *Earth Planets Space*, in press.

Okada, Y., Kasahara, K., Hori, S., Obara, K., Sekiguchi, S., Fujiwara, H. and Yamamoto, A. (2004). “Recent progress of seismic observation networks in Japan – Hi-net, F-net, K-NET and KiK-net–.” *Earth Planets Space*, Vol. 56, xv – xxviii.

Suzuki, W. and Iwata, T. (2007). “Source model of the 2005 Miyagi-Oki, Japan, earthquake estimated from broadband strong motions.” *Earth Planets Space*, Vol. 59, 1155 – 1171.